Dynamics of tightly focused femtosecond laser pulses in water

2013 Laser Phys. 23 106002

(http://iopscience.iop.org/1555-6611/23/10/106002)

IOP PUBLISHING LASER PHYSICS
Laser Phys. **23** (2013) 106002 (6pp) doi:10.1088/1054-660X/23/10/106002

Dynamics of tightly focused femtosecond laser pulses in water

S Sreeja[1,2], Ch Leela[1], V Rakesh Kumar[1], Suman Bagchi[1,3], T Shuvan Prashant[1,4], P Radhakrishnan[2], Surya P Tewari[1], S Venugopal Rao[1] and P Prem Kiran[1]

[1] Advanced Centre of Research in High Energy Materials (ACRHEM), University of Hyderabad, Hyderabad 500046, India
[2] International School of Photonics, Cochin University of Science and Technology, Cochin 682022, India

E-mail: svrsp@uohyd.ernet.in, premkiranuoh@gmail.com and prem@uohyd.ac.in

Received 4 July 2013
Accepted for publication 26 August 2013
Published 17 September 2013
Online at stacks.iop.org/LP/23/106002

Abstract
The dynamics of tightly focused ultrashort (40 fs) pulses manifested in terms of supercontinuum emission (SCE) and cavitation-induced bubbles (CIB) resulting from propagation in water over a wide range of input powers (6 mW–1.8 W) are presented. The effect of linear polarization (LP) and circular polarization (CP) on SCE in different external focal geometries ($f/6$, $f/7.5$ and $f/10$) is investigated and the results are discussed. SCE with higher efficiency and a considerable spectral blue shift is observed under tight focusing conditions ($f/6$) compared to loose focusing conditions ($f/10$). At higher input powers, CIB along the axis of propagation are observed to be assisting deeper propagation of these short pulses and enhanced SCE.

(Some figures may appear in colour only in the online journal)

1. Introduction

Since the initial observation of self-channeling of high-peak power femtosecond (fs) laser pulses in air by Braun *et al* [1], propagation of intense fs laser pulses (peak intensities $> 10^{12}$ W cm^{-2}) in different media has been an intriguing research area due to the interest in both fundamental science [2] and technological applications [3–5]. The propagation of intense fs pulses in transparent condensed media or gases is characterized by strong modification of its spatio-temporal profile due to the dynamic interplay between self-collapse of the laser pulse and the associated spectral broadening due to self-phase modulation (SPM) [6, 7]. The spectral manifestation of spatio-temporal modifications of focused laser beam in a medium results in a broad frequency sweep known as supercontinuum emission (SCE) extending, typically, from the ultraviolet to near-infrared spectral range [6]. SCE associated with filamentation of fs laser pulses occurs when the laser power (P) exceeds critical power (P_{cr}) for self-focusing in the medium [6, 7]. Potential applications of this phenomenon include optical pulse compression [8], fs-LIDAR and remote sensing [9]. Although the main mechanism responsible for SCE is believed to be self-focusing followed by SPM the evolution of SCE under different focusing conditions is not explored in great detail. Different mechanisms generate diverse components of the SCE/white light spectrum at certain spectral positions along the propagation direction of the pulse [6]. Self-steepening, space–time focusing plasma generated by multi-photon ionization, and four-wave mixing are also believed to play a significant role [6].

Despite a wide variety of applications envisaged, the generation of the SCE phenomenon due to filamentation has mainly been associated with long-range propagation of intense fs laser beams in a variety of media confined to either unfocused or loosely focused geometries [10–15].

[3] Present address: Raja Ramanna Centre for Advanced Technology, Indore, MP 452013, India.
[4] Present address: National University of Singapore, 2 Science Drive 3, 117542, Singapore.

A few recent attempts were directed towards understanding the ultrashort laser pulse filamentation [16–22] and the generated SCE at lower input powers [22, 23] with tightly focused beams. While many efforts were directed towards the achievement of spectrally flat SCE with a large blue shifted spectrum [24–28] the extent of blue shift from a medium has been reported to be constant due to the phenomenon of intensity clamping [14]. In view of (a) the recent observations of filamentation without intensity clamping [22], (b) interconnection between the spatial and spectral evolution of fs pulses in air under tight focusing conditions due to complete ionization of the medium [19–22, 29], (c) the observation of nonlinear interaction of fs pulses with water using high-angle Bessel beams depositing higher energy into the medium [30], and (d) the directional ejection of micro-bubbles [31], we investigated the spectral evolution of SCE from the propagation of tightly focused linearly polarized (LP) and circularly polarized (CP) 40 fs pulses in water over a wide range of input powers of 6 mW–1.8 W (corresponding to pulse energies of 6 μJ–1.8 mJ). The interesting role of cavitation induced bubbles (CIB) in enhancing the SCE with tight focusing geometries and at high input powers where intensity is clamped is discussed.

2. Experiment

A schematic illustration of the experimental setup for generating SCE from water is depicted in figure 1(a). Transform limited 40 fs, 800 nm *p*-polarized laser pulses at a repetition rate of 1 kHz (Coherent; Legend-USP) were focused into an 80 mm-long glass cuvette containing double distilled water. The amplifier was seeded with 15 fs pulses from an oscillator MICRA, Coherent, 1 W average power, 80 MHz repetition rate, 60 nm typical FWHM spectral width and 800 nm central wavelength. The input diameter ($1/e^2$) before the focusing element was 10 ± 0.1 mm. BK-7 plano-convex lenses of focal length 60 mm, 75 mm and 100 mm were used to achieve the focal geometries (numerical aperture (NA)) of $f/6$ (0.083), $f/7.5$ (0.066) and $f/10$ (0.05), respectively. For all the focusing geometries, the focus was ensured to be at an identical position within the cuvette.

An attenuator, a combination of a half wave plate (HWP) and a Brewster polarizer (BP), was used to vary the input pulse energy entering the medium. A quarter wave plate (QWP) was employed after the attenuator to change the polarization of the pulse. Part of the SCE generated was collected using a fiber optic coupled spectrometer (USB 4000, Ocean Optics) with a resolution of ~1.3 nm. A color CCD camera (SP620U, Ophir-Spiricon) synchronized with a laser pulse was used to image the self-emission and CIB from the propagating filament inside water and for estimating the diameter of the energy reservoir surrounding the filament inside the medium. A set of calibrated neutral density filters were placed in front of the spectrometer and CCD camera to avoid saturation of the sensor. The pulse duration of the incident and the transmitted 800 nm pulse were measured using '*Silhouette*' (Coherent, USA) based on the multi-photon intra-pulse interference phase scan (MIIPS) technique [32]. Appropriate adjustments

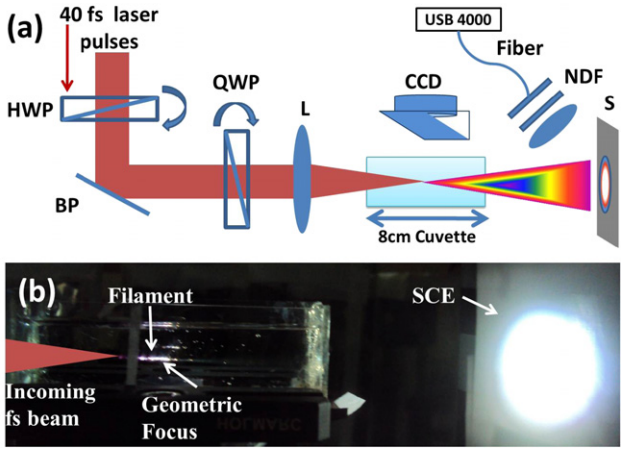

Figure 1. (a) Schematic illustration of the experimental setup for investigating SCE from double distilled water using focused fs pulses. HWP—half wave plate, BP—Brewster polarizer in the reflection mode, QWP—quarter wave plate, L—lens, C—cuvette, S—screen, NDF—neutral density filter and CCD—camera. (b) Side view of the filament within the cuvette and the SCE generated with $f/6$ focusing geometry at 1.2 W P_{abs} for LP pulses.

were made with the laser compressor gratings to ensure that the final pulse duration entering the water cuvette was indeed 40 fs.

SCE spectra were collected for 350 laser shots to reduce the noise from pulse to pulse fluctuations. The experiment was performed for both LP and CP pulses over the power range of 6 mW–1.8 W (energy range of 6 μJ–1.8 mJ per pulse). The power of the incident transmitted 800 nm pulses and the SCE were measured using a power meter (Coherent, PM30). The power entering the medium post Fresnel losses (due to the focusing lens, the entrance face of the cuvette and the cuvette–water interface) was considered as the input power (P_{abs}) for all calculations. We observed that 68–70% of the incident laser power was absorbed by the medium. The efficiency of the SCE (η_{SCE}) was estimated as P_{SCE}/P_{abs}. A 800 nm filter was used to cut off the transmitted input laser pulses after the cuvette while measuring the efficiency of SCE. The critical power for self-focusing is calculated from the equation $P_{cr} = 3.77\lambda^2/8\pi n_0 n_2$, where λ is the central wavelength, and n_0 and n_2 are the linear and nonlinear refractive indices, respectively [6]. The P_{cr} for water is taken as 4.4 MW [33].

3. Results and discussion

Figure 1(b) shows an image of a typical filament propagating inside water and the associated SCE at an input power of 1.25 W for LP pulses in the $f/6$ focusing geometry. The filamentation is observed to start ahead of the geometrical focus for all the three focusing geometries. The filaments were propagating for over 15–53 mm inside the cuvette corresponding to 74–84 Z_0, where Z_0 is the Rayleigh range of focusing geometries used in the present study. The fs pulses propagating in water produced SCE with conical colored rings at low input powers and SCE with a predominantly white colored central portion was observed at higher input powers

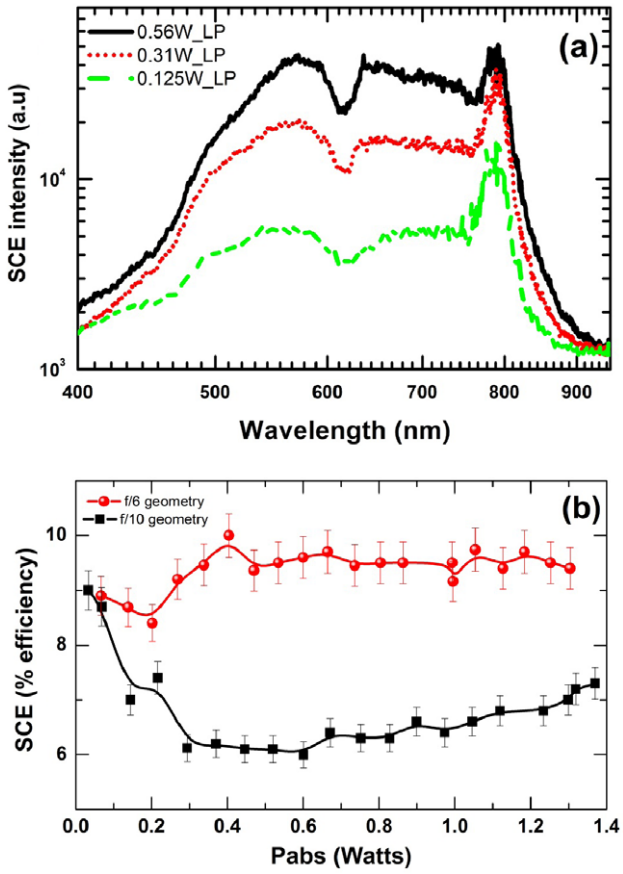

Figure 2. (a) SCE spectra with LP pulses obtained in $f/7.5$ focal geometry at an input power of 0.125, 0.31 and 0.56 W. The data are plotted in logarithmic scale for convenient comparison. (b) Variation of SCE efficiency (%) with absorbed power P_{abs} for $f/6$ (—●—), and $f/10$ (. . . ■ . . .) focusing geometries. Solid lines are guides to the eye.

(figure 1(b)). Figure 2(a) shows the SCE spectrum recorded at different input powers with $f/7.5$ focusing geometry. The spectra demonstrated broadening towards both sides of the central wavelength. The symmetrical spectral broadening about the incident laser wavelength (800 nm) is ascribed to the Kerr nonlinearity induced SPM. The asymmetric component in the blue spectral region occurs due to processes such as space–time focusing, self-steepening, [34] and plasma formation that arise from free electrons generated through multi-photon ionization (MPI) in gases and multi-photon excitation (MPE) in condensed media [6]. In addition to the asymmetric broadening there is a marked dip near 611 nm superimposed on the white light continuum corresponding to an inverse Raman effect due to the –OH stretching bond (3650 cm^{-1}) [25, 26, 35] of water. The Raman dip intensity increased with increasing excitation energy indicating the participation of more water molecules in the process as more of the excitation energy was converted into Raman modes. The SCE spectrum (figure 2(a)) shows a flat response in the 550–750 nm spectral range except for the inverse Raman dip at 611 nm. The SCE spectrum is nearly flat over the 500–750 nm range and for different P_{abs} used. Figure 2(b) shows the efficiency of the SCE with LP pulses for $f/6$ and $f/10$ focusing geometries. SCE with an efficiency of ∼7% and ∼10% was observed with $f/10$ and $f/6$ focusing geometries, respectively. With increasing NA from 0.05 ($f/10$) to 0.083 ($f/6$) the η_{SCE} was observed to increase by 1.5 times indicating higher conversion efficiency. The spectral flatness also increased with increasing numerical aperture (NA) and input powers. However, the flatness reduced slightly with CP pulses compared to that of LP pulses. The SCE spectra for different focal geometries of $f/6$ and $f/10$ at an absorbed power of 1.2 W for CP pulses are shown in figure 3. The spectra illustrate noticeable enhancement in both the symmetric and asymmetric branches of SCE for tight focusing geometry. Tighter focusing in the case of $f/6$ geometry has resulted in increased conversion of incident laser pulse energy into SCE, especially towards the blue side of the spectrum indicating the role of tighter focusing on the evolution of SCE spectrum in terms of increased peak intensity near the focal plane. As input polarization of the pulse was changed from LP to CP (simply by rotating the quarter wave plate), a reduction in the SCE intensity for all the three focusing geometries is observed at lower input powers which is in good agreement with earlier reports [35]. However, with increasing input powers the difference in SCE from LP and CP pulses is observed to be negligible due to the increased presence of the CIB along the propagation direction. The ratio (1.5) of the critical powers for self-focusing with LP and CP pulses accounts for MPE being less efficient for CP pulses [6]. For a given NA, the ratio of SCE intensities for CP and LP pulses (SCE_{CP}/SCE_{LP}) as a function of wavelength is always less than 1, confirming the suppression of SCE with CP pulses in contrast to LP pulses.

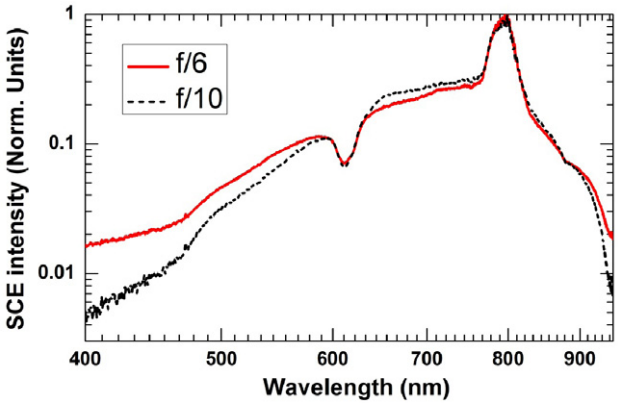

Figure 3. SCE spectra from water with $f/6$ (red, solid line) and $f/10$ (black, dashed line) focusing geometries at P_{abs} of 1.2 W for CP pulses.

The blue edge of the SCE spectrum, i.e., the minimum cutoff wavelength (λ_{min}) or maximum positive frequency shift (ω_{max}) as a function of the input laser power from the collected SCE spectra, is found to decrease continuously with increasing input powers for all the focusing geometries. Figure 4(a) shows the variation of λ_{min} for both $f/6$ and $f/10$ focusing geometries for LP pulses. At lower input powers (<30 mW) the λ_{min} is almost the same for both the focusing geometries and the separation has become

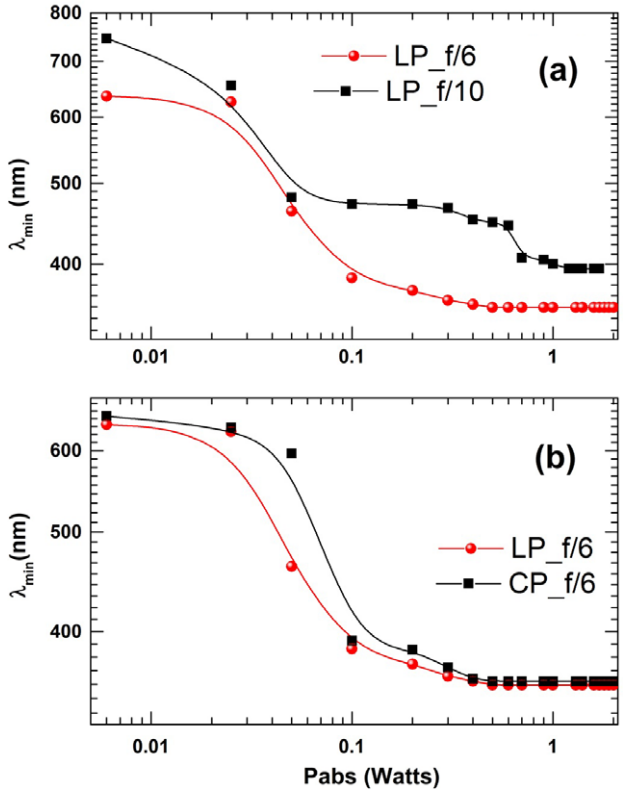

Figure 4. Variation of minimum wavelength (λ_{min}) with absorbed power P_{abs} for (a) $f/6$ and $f/10$ focusing geometries for LP pulses. (b) LP and CP pulses in $f/6$ focusing geometry. Solid lines are guides to the eye.

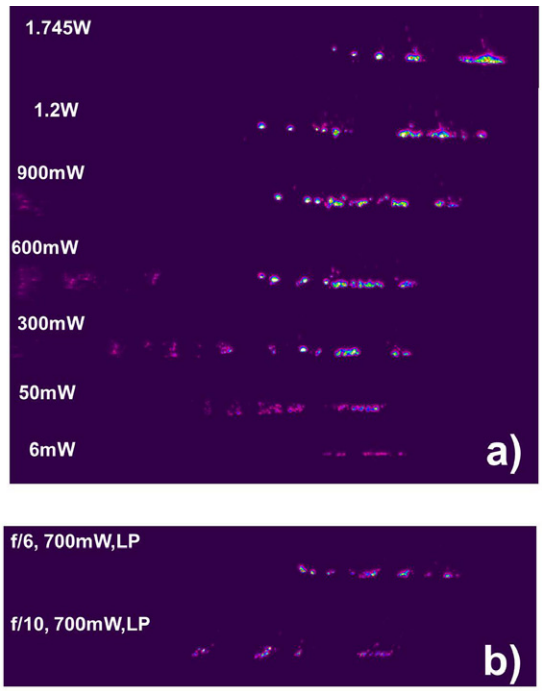

Figure 5. Image of the CIB observed in water during the propagation of 40 fs pulses (a) at different P_{abs} under $f/6$ focusing geometry (b) comparison of the CIB under $f/6$ and $f/10$ focusing geometries.

considerable (∼100 nm) over the 50 mW–600 W input power range. The λ_{min} was found to be blue shifted for $f/6$ focusing geometry compared to $f/10$ focusing geometry at input powers >50 mW. This clearly demonstrates the presence of higher intensities in the vicinity of the interaction region (focal plane) for $f/6$ focusing geometry while also revealing the blue shift of the SCE spectra due to the external focusing of the fs pulses inside transparent media. With increasing input powers, λ_{min} has shown interesting evolution. Under $f/6$ focusing geometry, the λ_{min} decreased in two rates of P_{abs} before and after 100 mW, while for $f/10$ focusing geometry, the transition occurred in three different power regimes of 6–50 mW, 100–600 mW and beyond 600 mW. A similar blue shift of SCE was observed in the SCE from air using tight focusing conditions [22] though the variation of λ_{min} observed in water was small compared to that observed in air, because air molecules can be completely ionized without being opaque [20]. Although plasma electron densities of about 7×10^{20} cm^{-3}, which increase with tighter focusing geometry, were observed in numerical simulations (in a tight focusing geometry of $f/3.4$ and at pulse energies of 4 μJ [22]), the complete ionization of the medium at high input powers without being opaque needs further exploration due to the higher number density (10^{22} cm^{-3} at 1 atmosphere compared to that of 10^{19} cm^{-3} in air) in spite of the optical bandgap and the order of MPI being less than that of air. However, λ_{min} has become constant with increasing input powers above 300 mW and 700 mW in $f/6$ and $f/10$ focusing geometries, respectively, indicating the presence of intensity clamping which is ∼1 TW cm^{-2} for water. This intensity is sufficient to cause the breakdown of water and cause CIB near the focal plane (within the interaction region) of the laser pulse inside water [36].

The evolution of CIB was studied by capturing the self-emission from the wake of fs pulses/filaments propagating in water (figure 5). Higher intensity and brighter SCE in the $f/6$ geometry compared to that of $f/10$ geometry clearly indicates the presence of interesting dynamics inside the medium. Moreover, λ_{min} for $f/6$ geometry was always blue shifted compared to that with $f/10$ geometry (figure 4(a)). Notably, the separation of blue shift between the focusing geometries increased with increasing input powers (figure 4(a)). This behavior was more dominant beyond P_{abs} of 100 mW, where the onset of CIB was observed for the focusing geometries used. At lower input powers, η_{SCE} was observed to be similar (∼9%) for all focusing conditions (figure 2(b)). With a gradual increase of P_{abs}, an interesting dependence of η_{SCE} on focusing conditions was observed. For $f/6$ focusing geometry η_{SCE} has remained almost constant, while for $f/10$ it decreased quite significantly to 6%. The difference in the η_{SCE} has become more obvious above P_{abs} ∼300 mW (30 μJ). Incidentally, the CIB is more obvious around 300 mW. The separation between the CIB at different points along the propagation direction decreased with increasing input power (figure 5(a)) and increasing NA (figure 5(b)). We believe that the micron-sized CIB [5, 37] along the propagation direction act like tiny spherical lenses for filament propagation

by refocusing the diverging laser energy and the trailing edge of the pulse along the propagation axis overcoming the diffraction. This leads to increasing deposition of laser energy during the propagation of fs pulses and the enhanced SCE in the wake of fs pulses. The observed anomalous increase in the λ_{min} beyond the clamping intensity seems to originate from the plasma evolution around the focal plane. Moreover, the trailing part of fs pulses was observed to support higher intensities during filamentation [38]. The CIB, due to fs pulses, were observed to live up to few tens of ns with energy-dependent sub-micron to micron diameters [5, 37]. Though the CIB and their interaction is a hydrodynamic phenomenon lasting less than 1 ms which is relatively slow when compared to the ultrafast processes occurring later in the wake of the fs pulse, the laser-produced plasma starts expanding within 20 ps due to electron–ion energy transfer time, effectively inducing a temperature above 200 °C due to the ultrafast phase transitions [39]. The formation of CIB due to fs laser pulses is observed to be a very dynamic process below and above the breakdown threshold of the medium with a typical free electron density of $\sim 3.5 \times 10^{20}$ cm^{-3} at the end of the laser pulse [5]. Beyond the threshold energy the CIB progresses as explosive vaporization due to phase explosion with peak focus temperatures >300 °C [5]. The phenomenon of CIB in water due to fs pulses is observed to start at intensities higher than TW cm^{-2} [36, 40] and is strongly dependent on the pulse energy and duration and repetition rate [37]. The plasma shielding effect that counters the propagation of laser pulses inside the medium is observed to reduce as the incident pulse duration becomes shorter [36].

We also strongly believe that in the tight focusing geometry, the initial high beam curvature, due to external focusing, leads to a higher degree of ionization of the medium, leading to dynamically interacting CIB acting like a series of spherical lenses which in turn prevent plasma defocusing from playing any significant role in the intensity clamping [5, 22]. A similar phenomenon corresponding to the fully ionized medium with electron density up to 2×10^{19} cm^{-3} in filamentation in air under similar focusing conditions (NA of 0.11) and in the range of 10^{18}–10^{19} cm^{-3} for NA of 0.08 [20–22, 39–41] due to the external tight focusing conditions, was recently reported. In condensed media such as water or solids the phenomenon is expected to be totally different due to low ionization thresholds and higher densities. Many other phenomena such as (i) the propagation of tightly focused fs pulses inside water [30, 31], (ii) ionization, plasma shielding and breakdown phenomena of water at intensities greater than TW cm^{-2} within the filament [36, 40], (iii) the effect of pulse splitting [29] and (iv) interaction of the cavitation bubbles in water [30, 31, 42, 43] with high repetition rate pulses need to be understood completely so as to devise practical high-intensity SCE sources.

4. Conclusion

In summary, the effects of external tight focusing conditions on the evolution of SCE resulting from the propagation of 40 fs laser pulses in water is studied in detail. A flat SCE with increased efficiency was observed with tightly focused fs pulses. The SCE from tight focusing geometry was always higher than the loose focusing geometry for both LP and CP pulses. For tighter focusing geometries, however, the minimal cutoff wavelength (λ_{min}) for the SCE got saturated at higher input powers, and CIB along the propagation axis is observed to assist further propagation of fs pulses, thereby generating enhanced SCE. This makes it possible to stretch the intensity levels of fs pulses inside the medium beyond the clamping value. Controlled deposition of laser energies around the focal region with tighter focusing conditions is an interesting way of generating enhanced SCE which paves a path for novel intense sources of radiation and several possible practical applications.

Acknowledgments

Financial support from DRDO is gratefully acknowledged. SS acknowledges the JRF from UGC, India. The authors thank Dr Arnaud Couairon and Dr C L Arnold for valuable discussions.

References

[1] Braun A, Korn G, Liu X, Du D, Squier J and Mourou G 1995 *Opt. Lett.* **20** 73
[2] Belgiorno F, Cacciatori S L, Ortenzi G, Sala V G and Faccio D 2010 *Phys. Rev. Lett.* **104** 140403
[3] D'Amico C, Houard A, Akturk S, Liu Y, Le Bloas J, Franco M, Prade B, Couairon A, Tikhonchuk V T and Mysyrowicz A 2008 *New J. Phys.* **10** 013015
[4] Wang T-J, Marceau C, Yuan S, Chen Y, Wang Q, Théberge F, Châteauneuf M, Dubois J and Chin S L 2011 *Laser Phys. Lett.* **8** 57
[5] Vogel A, Linz N, Freidank S and Paltauf G 2008 *Phys. Rev. Lett.* **100** 038102
[6] Couairon A and Mysyrowicz A 2007 *Phys. Rep.* **441** 47
[7] Boyd R W, Lukishova S G and Shen Y R 2009 *Self-focusing: Past and Present: Fundamentals and Prospects* (New York: Springer) chapter 1
[8] Schulz E, Binhammer T, Steingrube D S, Rausch S, Kovacev M and Morgner U 2009 *Appl. Phys.* B **95** 269
[9] Kasparian J *et al* 2003 *Science* **301** 61
[10] Eisenmann S, Pukhov A and Zigler A 2007 *Phys. Rev. Lett.* **98** 155002
[11] Fibich G and Ilan B 2002 *Phys. Rev. Lett.* **89** 013901
[12] Méchain G, Couairon A, Franco M, Prade M and Mysyrowicz A 2004 *Phys. Rev. Lett.* **93** 035003
[13] Varela O, Zair A, Roman J S, Alonso B, Sola I J, Prieto C and Roso L 2009 *Opt. Express* **17** 3630
[14] Liu W, Petit S, Becker A, Akozbek N, Bowden C M and Chin S L 2002 *Opt. Commun.* **202** 189
[15] Mizeikis V, Juodkazis S, Balciunas T, Misawa H, Kudryashov S I, Zvorykin V D and Ionin A A 2009 *J. Appl. Phys.* **105** 123106
[16] Sudrie L, Couairon A, Franco M, Lamouroux B, Prade B, Tzortzakis S and Mysyrowicz A 2002 *Phys. Rev. Lett.* **89** 186601
[17] Couairon A, Sudrie L, Franco M, Prade B and Mysyrowicz A 2005 *Phys. Rev.* B **71** 125435
[18] Théberge F, Liu W, Simard P T, Becker A and Chin S L 2006 *Phys. Rev.* E **74** 036406
[19] Ionin A A, Kudryashov S I, Makarov S V, Seleznev L V and Sinitsyn D V 2009 *JETP Lett.* **90** 423
[20] Kiran P P, Bagchi S, Krishnan S R, Arnold C L, Kumar G R and Couairon A 2010 *Phys. Rev.* A **82** 013805

[21] Liu X-L, Lu X, Liu X, Xi T-T, Liu F, Ma J-L and Zhang J 2010 *Opt. Express* **18** 26007
[22] Kiran P P, Bagchi S, Arnold C L, Krishnan S R, Kumar G R and Couairon A 2010 *Opt. Express* **18** 21504
[23] Liu W, Kosareva O, Golubtsov I S, Iwasaki A, Becker A, Kandidov V P and Chin S L 2003 *Appl. Phys.* B **76** 215
[24] Srinivas N K M N, Harsha S S and Rao D N 2005 *Opt. Express* **13** 3224
[25] Moghaddam M R A, Harun S W, Akbari R and Ahmad H 2011 *Laser Phys. Lett.* **8** 369
[26] Buczynski R, Pysz D, Stepien R, Waddie A J, Kujawa I, Kasztelanic R, Franczyk M and Taghizadeh M R 2011 *Laser Phys. Lett.* **8** 443
[27] Dharmadhikari A K, Rajgara F A and Mathur D 2006 *Appl. Phys.* B **82** 575
[28] Wang L, Fan Y-X, Yan Z D, Wang H-T and Wang Z-L 2010 *Opt. Lett.* **35** 2925
[29] Papazoglou D G and Tzortzakis S 2008 *Appl. Phys. Lett.* **93** 041120
[30] Faccio D, Rubino E, Lotti A, Couairon A, Dubietis A, Tamošauskas G, Papazoglou D G and Tzortzakis S 2012 *Phys. Rev.* A **85** 033829
[31] Faccio D, Tamošauskas G, Rubino E, Darginavičius J, Papazoglou D G, Tzortzakis S, Couairon A and Dubietis A 2012 *Phys. Rev.* E **86** 036304
[32] Xu B, Gunn J M, Cruz J M D, Lozovoy V V and Dantus M 2006 *J. Opt. Soc. Am.* B **23** 750
[33] Brodeur A and Chin S L 1998 *Phys. Rev. Lett.* **80** 4406
[34] Gaeta A L 2000 *Phys. Rev. Lett.* **84** 16
[35] Sandhu A S, Banerjee S and Goswami D 2000 *Opt. Commun.* **181** 101
[36] Hammer D X, Jansen E D, Frenz M, Noojin G D, Thomas R J, Noack J, Vogel A, Rockwell B A and Welch A J 1997 *Appl. Opt.* **36** 5630
[37] Tiwari D, Bellouard Y, Dietzel A, Ren M, Rubingh E and Meinders E 2010 *Appl. Phys. Express* **3** 127101
[38] Sun X, Xu S, Zhao J, Liu W, Cheng Y, Xu Z, Chin S L and Mu G 2012 *Opt. Express* **20** 4790
[39] Shaffer C B, Nishimura N, Glezer E N, Kim A M-T and Mazur E 2002 *Opt. Express* **10** 196
[40] Geints Yu E and Zemlyanov A A 2011 *Atmos. Oceanic Opt.* **24** 144
[41] Vogel A, Noack J, Nahen K, Theisen D, Busch S, Parlitz U, Hammer D X, Noojin G D, Rockwell B A and Birngruber R 1999 *Appl. Phys.* B **68** 271
[42] Minardi S, Gopal A, Tatarakis M, Couairon A, Tamosaukas G, Piskarskas R, Dubietis A and Trapani P D 2008 *Opt. Lett.* **33** 86
[43] Tinne N, Schumacher S, Nuzzo V, Arnold C L, Lubatschowski H and Ripken T 2010 *J. Biomed. Opt.* **15** 068003